

## Analytical modeling of non-Fickian wave-diffusion of gas in heterogeneous media



Maurice L. Rasmussen<sup>a</sup>, Faruk Civan<sup>b,\*</sup>

<sup>a</sup> School of Aerospace and Mechanical Engineering, The University of Oklahoma, Norman, OK 73019, USA

<sup>b</sup> Mewbourne School of Petroleum and Geological Engineering, The University of Oklahoma, Norman, OK 73019, USA

### ARTICLE INFO

#### Article history:

Received 31 January 2013

Received in revised form 7 March 2014

Accepted 8 July 2014

Available online 22 July 2014

The coauthor dedicates this paper to the memory of David Ross Boyd Professor Emeritus Maurice L. Rasmussen, a great mathematician, a creative and practical engineer, an outstanding researcher, and a dedicated teacher.

#### Keywords:

Non-Fickian

Wave-diffusion

Gas dissolution

High-pressure

Heterogeneous medium

Full-, short-, and long-time analytical solutions

### ABSTRACT

An isothermal transient-state non-Fickian diffusion model is developed and analytically solved for description of gas dissolution in locally heterogeneous media suddenly exposed to a high pressure gas. The full-, short-, and long-time analytical solutions are used to establish the significance of the non-Fickian gas dissolution in heterogeneous media compared to the Fickian diffusion assumption. Parametric studies are carried out by means of the special analytical-solutions obtained for gas transport in the semi-infinite and finite-thickness heterogeneous media involving a delay time. The profiles of concentration and diffusion flux obtained for the non-Fickian wave-diffusion case are compared with the Fickian pure-diffusion case. The initial propagation of a right-running wave and its reflection from the wall are illustrated for the concentrations and diffusion fluxes. The small-time behavior is shown to be inherently wave-like and the discontinuity wave front propagates into the medium with the speed decreasing with time. For small times, the differences between the wave- and pure-diffusion cases are found to be significant depending on the magnitude of the delay time. For sufficiently large times, the wave behavior dies out and the wave solutions approach the equilibrium pure-diffusion solutions, except very near the decaying wave front. The formulations presented in this paper are of practical importance because they can be instrumental in determination of the diffusivity, interface surface mass-transfer coefficient, and rate of dissolution of gases in heterogeneous medium. A parameter estimation method is also proposed and elaborated for estimation of the diffusion and interface surface mass-transfer coefficients from measured pressure decay data.

© 2014 Elsevier Inc. All rights reserved.

## 1. Introduction

Modeling of gas dissolution in a locally heterogeneous medium is a complicated task which results with wave diffusion because of non-Fickian transport involving time delay. Various examples of practical importance can be found in the natural and engineering systems where the non-Fickian effects should be considered for accurate description and proper modeling [1–4]. For example, Das [5] emphasizes that the behavior of some systems such as the Brownian species motion in a potential field, the ionic species diffusion in superionic conductors under inertial effect, and the neutron diffusion in nuclear reactors,

\* Corresponding author. Address: Mewbourne School of Petroleum and Geological Engineering, University of Oklahoma, T 1210 Sarkeys Energy Center, 100 East Boyd St., Norman, OK 73019-1003, USA. Tel.: +1 (405) 325 6778; fax: +1 (405) 325 7477.

E-mail address: [fcivan@ou.edu](mailto:fcivan@ou.edu) (F. Civan).

## Notation

$A$	cross-sectional area of the test tank, $L^2$
$D$	gas diffusivity in the heterogeneous medium, $L^2/T$
$c$	gas mass concentration of the heterogeneous medium, $M/L^3$
$H$	thickness of the gas column, $L$
$J$	gas mass flux, $M/L^2/T$
$k$	interface mass-transfer coefficient, $L/T$
$L$	thickness of the heterogeneous medium, $L$
$M$	molecular weight of gas, $M/mol$
$p$	pressure, $M/L/T^2$
$Q$	cumulative gas mass, per unit cross section area, dissolved in the heterogeneous medium, $M/L^2$
$R$	universal gas constant, $ML^2/mol/\theta/T^2$
$x$	distance measured from the gas–heterogeneous medium interface into the heterogeneous medium, $L$
$t$	time, $T$
$T$	temperature, $\theta$
$x$	distance measured from the gas–heterogeneous medium interface, $L$
$v$	$\sqrt{D/\tau}$ , wave speed of sound, $L/T$
$V$	volume, $L^3$
$w$	gas mass fraction of the heterogeneous medium, dimensionless
$Z$	real-gas deviation factor, dimensionless

### Greek

$\beta$	isothermal coefficient of expansion, dimensionless
$\tau$	delay time, $T$
$\rho$	density, $M/L^3$
$\lambda$	root of Eq. (3.21), dimensionless
$\phi$	fugacity coefficient of the dissolving gas in the heterogeneous medium, dimensionless

### Subscripts

$D$	dimensionless
$g$	gas
LT	long-time
ST	short-time
o	initial or reference state

### Superscripts

*	equilibrium state
---	-------------------

and the associated species fluxes at absorbing boundaries, can be described adequately by a non-Fickian type diffusion equation.

The conventional Fickian law of diffusion describes the spontaneous transport of species in a carrying-medium because of concentration gradients under the conditions of local thermodynamic equilibrium. A medium is considered at local thermodynamic equilibrium only when its constituents are at equilibrium with each other. This requires the fulfillment of two critical conditions. First, a medium under external factors should be able to approach equilibrium much faster than its macro parameters and, second, the relaxation to local equilibrium should occur sufficiently faster than relaxation to global equilibrium [2,3]. Thus, the conventional Fickian model cannot describe a wave-like transfer of species mass by diffusion involving a time delay (relaxation) in heterogeneous medium because often these conditions are not fulfilled. The relaxation time induces traveling jump discontinuities in diffusing species mass concentration profiles. Such behavior has been observed in various non-Fickian transfer processes [6]. However, the non-Fickian conditions are mostly prevalent for short-times but disappear later for long-times as attested by the analyses carried out by Chen and Liu [7] and in the present paper.

The internal structure of some heterogeneous medium may cause considerable retardation in the flux of diffusing species because it requires a certain amount of time, referred to as delay or relaxation time, in order to attain a local thermodynamic equilibrium. Under such conditions, attaining local thermodynamic equilibrium is not an instantaneous but a gradual process because of delay in the flux caused by the different scales (for example, nano, micro, or medium types) of the various internal features existing in heterogeneous medium, such as pointed out by Civan and Slepcevich [8] and Civan [9] for freezing and thawing of moist soils. Consequently, several studies, including by Abarzhi [3] and Liu et al. [10], have demonstrated that the conventional Fickian law of diffusion is incapable of describing the diffusion phenomenon in locally nonequilibrium medium. For example, the natural and synthetic fibrous materials have been reported to indicate sharp fronts in dye

concentration profiles encountered during the dyeing of these materials for coloring [11]. The diffusion of water in polymers such as crosslinked melamine-formaldehyde resins is another example of transfer by non-Fickian diffusion [12].

In this paper, also, we show theoretically that such sharp fronts can indeed result from the nature of the non-Fickian wave diffusion phenomenon by modeling and solving analytically the process of gas dissolution in heterogeneous medium. In fact, we demonstrate that the slopes of the straight-lines obtained for the small- and large-time analytical solutions of the non-Fickian model on semi-log coordinates are different. This type of break in the slopes has been observed also experimentally by Smith and Fisher [12] for polymer in water at 95 °C and by Shankar [13]. Hence, this characteristic behavior of the non-Fickian diffusion processes can be facilitated for estimation of the diffusion and interface surface mass-transfer coefficients from measured pressure decay data based on our analytical solution.

The analytical solution and applications for the gas transfer by equilibrium pure-diffusion in homogeneous medium brought to sudden contact with gas were presented elsewhere by Civan and Rasmussen [14,15] and Rasmussen and Civan [16]. Comprehensive reviews of the relevant equilibrium diffusion studies were also presented there, which are not repeated here. They demonstrated the application of their methodology for rapid and effective determination of the film-mass-transfer and diffusion coefficients from time-limited experimental data obtained by the pressure-decay method under equilibrium conditions considered for conventional analysis and interpretation of the standard laboratory pressure-decay tests.

This paper presents some extensions over the previous studies of Civan and Rasmussen [4,14,15] to account for the non-Fickian effects in heterogeneous medium. This may be useful for future work dealing with the interpretation of the results of tests involving conditions of isothermal wave-diffusion with delay. Thus, an attempt is made at formulation and analytical solution of the non-Fickian wave-diffusion phenomenon and demonstration of its significance and implications by solving a problem involving gas dissolution with delay in heterogeneous medium suddenly contacted with a high pressure gas. A model for non-Fickian diffusion and transport of a single gas component in heterogeneous medium under isothermal conditions and subject to the resistance of the interface between the gas and the carrying-medium to gas dissolution is developed and solved analytically. The importance of the non-Fickian wave-diffusion in heterogeneous medium in comparison to the Fickian pure-diffusion assumption of conventional approaches is emphasized by means of the full-, short-, and long-time analytical solutions. Effect of the delay time is investigated by means of the parametric studies carried out using the special analytical solutions obtained for gas transport in semi-infinite and finite-thickness heterogeneous media. We show that the small-time behavior is wave-like with a discontinuity wave front propagating into the medium with a speed decreasing with time and the significance of the differences between the wave-diffusion and the pure-diffusion cases depend on the value of the delay time. For sufficiently large times, nevertheless, the wave behavior diminishes and the wave solutions approach the equilibrium pure-diffusion solutions, except for very near the decaying wave front.

A parameter estimation method is also proposed and elaborated for estimation of the diffusion and interface surface mass-transfer coefficients from measured pressure decay data. This is accomplished by virtue of the straight-line plots obtained from the small- and large-time analytical solutions of the non-Fickian model on semi-log coordinates. The characteristic break determined in the slopes of the straight-lines for the small- and large-times is facilitated based on our analytical solutions for estimation of the diffusion and interface surface mass transfer coefficients from measured pressure decay data obtained similar to Civan et al. [17,18] by the pressure decay tests.

In summary, the overall objective of this paper is to develop the analytical background required for description of the non-Fickian gas dissolution in heterogeneous medium and propose a method for estimation of the parameters such as the diffusion and interface surface mass-transfer coefficients from measured pressure decay data. However, applications for certain specific cases are deferred to future studies.

## 2. Modeling non-Fickian gas dissolution in heterogeneous medium

Consider a heterogeneous medium brought into contact with a pure high-pressure gas instantly at isothermal conditions in a closed tank. The formulation is presented for gas diffusion with delay in a one-dimensional heterogeneous medium.

### 2.1. Gas-phase equations

Assuming equilibrium in the gas phase, the gas properties are considered uniform throughout the gas phase but vary with time during the pressure-decay tests. Because the gas phase is a single component system, its gas component mass concentration  $c_g$  and density  $\rho_g$  are the same; i.e.  $c_g = \rho_g$ . The real gas equation of state is applied to express the gas density  $\rho_g$  as:

$$\rho_g = \frac{M_g p}{ZRT}, \quad (2.1)$$

where  $M_g$  denotes the molecular weight, and  $p$  and  $T$  are the pressure and temperature of the gas,  $R$  is the universal gas constant, and  $Z = Z(p, T)$  represents the real gas deviation factor, correlated empirically as a function of the reduced pressure and temperature in the literature. The volume  $V$  and mass  $m$  of the gas phase are given, respectively, by:

$$V = AH, \quad (2.2)$$

$$m = \rho_g V, \quad (2.3)$$

where  $A$  and  $H$  denote the cross-sectional area and the thickness of the test tank containing the gas column contacting a heterogeneous medium into which gas diffuses. If  $J$  denotes the mass flux of the gas diffusing from the gas phase into the heterogeneous medium at the interface, the gas phase mass balance is given by:

$$\frac{dm}{dt} = -AJ|_{x=0}, \quad t > 0, \quad (2.4)$$

where  $t$  is time and  $x$  is the distance measured from the contact surface between the gas and the heterogeneous medium. The initial gas mass is given by:

$$m = m_0, \quad t = 0. \quad (2.5)$$

Hence, solving Eqs. (2.4) and (2.5) yields:

$$\frac{m_0 - m}{A} = \int_0^t J|_{x=0} dt = Q(t), \quad t > 0, \quad (2.6)$$

where  $Q$  denotes the cumulative mass of gas dissolved in the heterogeneous medium per unit cross-section area  $A$  of the interface between the gas and heterogeneous medium. Thus, substituting Eqs. (2.1)–(2.3) into Eq. (2.6) yields a gas phase mass balance equation as:

$$\frac{M_g H}{RT} \left[ \frac{p_0}{Z_0} - \frac{p}{Z} \right] = Q(t), \quad t > 0. \quad (2.7)$$

An alternative expression to Eq. (2.6) for  $Q(t)$  can be derived. Let  $c(x, t)$  be the concentration (mass per unit volume) of the gas that is dissolved in the heterogeneous medium, and let  $c_0$  be its initial value. Then  $Q$  can be expressed as:

$$Q(t) = \int_0^L [c(x, t) - c_0] dx, \quad (2.8)$$

where  $L$  is the thickness of the heterogeneous medium. The function  $Q(t)$  can be interpreted as the average gas accumulation in the heterogeneous medium, measured per unit area of the interface cross section.

## 2.2. Non-Fickian gas diffusion in heterogeneous medium

The mass concentration  $c$  and mass fraction  $w$  of the gas component in the incompressible heterogeneous medium are related by:

$$c = \rho w, \quad (2.9)$$

where  $\rho$  denotes the density of the heterogeneous medium.

The conservation of the dissolved gas mass in the heterogeneous medium is given by neglecting the convective transport as:

$$\frac{\partial c}{\partial t} + \frac{\partial J}{\partial x} = 0, \quad 0 \leq x \leq L, \quad t > 0. \quad (2.10)$$

The constitutive equation for mass flux of the dissolved gas  $J$  is given by:

$$\tau \frac{\partial J}{\partial t} + J = -\rho D \frac{\partial w}{\partial x} = -\rho D \frac{\partial(c/\rho)}{\partial x} = -D \frac{\partial c}{\partial x}, \quad 0 \leq x \leq L, \quad t > 0, \quad (2.11)$$

where  $D$  is the coefficient of diffusion, and  $\tau$  is a delay time [3]. When  $\tau = 0$ , Eq. (2.11) reduces to Fick's law.

We assume a constant diffusion coefficient; i.e.  $D \cong \text{constant}$  and an incompressible heterogeneous medium. Then, Eqs. (2.10) and (2.11) can be manipulated to eliminate either  $c$  or  $J$  in favor of the other to obtain:

$$\tau \frac{\partial^2 c}{\partial t^2} + \frac{\partial c}{\partial t} = D \frac{\partial^2 c}{\partial x^2}, \quad 0 \leq x \leq L, \quad t > 0 \quad (2.12)$$

and

$$\tau \frac{\partial^2 J}{\partial t^2} + \frac{\partial J}{\partial t} = D \frac{\partial^2 J}{\partial x^2}, \quad 0 \leq x \leq L, \quad t > 0. \quad (2.13)$$

Eqs. (2.12) and (2.13) are damped-wave equations, referred to as the telephone or telegraph equations. The characteristic wave speed is equal to

$$v = \sqrt{D/\tau}. \quad (2.14)$$

### 2.3. Conditions of solution for equations

The initial conditions are given by:

$$c = c_0, \quad \frac{\partial c}{\partial t} = 0, \quad J = 0, \quad \frac{\partial J}{\partial t} = 0, \quad 0 \leq x \leq L, \quad t = 0. \quad (2.15)$$

The value of the diffusing gas mass flux  $J|_{x=0}$  at the interface, as well as the concentration  $c$  of the gas that has been absorbed by the heterogeneous medium, can be determined by solving the transient-state gas diffusion model for the heterogeneous medium.

The interface resistive or hindered gas mass-transfer boundary condition is given by:

$$J|_{x=0} = k(c^* - c), \quad x = 0, \quad t > 0, \quad (2.16)$$

where  $k$  is the film mass-transfer coefficient at the interface. The symbol  $c^*$  denotes the saturation or equilibrium gas concentration of the heterogeneous medium. The sealed boundary condition prevailing at the bottom of the heterogeneous medium is given by:

$$J = 0, \quad x = L, \quad t > 0. \quad (2.17)$$

### 2.4. Practical considerations for solution of equations

In the following sections, we determine the solutions of Eqs. (2.12) and (2.13) together with the initial and boundary conditions given by Eqs. (2.15)–(2.17) for the non-Fickian gas transport in heterogeneous medium. The analytical solutions are obtained for semi-infinite ( $L \rightarrow \infty$ ) and finite-thickness ( $L = \text{prescribed}$ ) regions. The semi-infinite solution can be used when the diffusivity coefficient or time is so small that the gas cannot progress very far from the gas–heterogeneous medium interface into the heterogeneous medium and cannot effectively reach the impermeable bottom of the heterogeneous medium placed in a test tank within the test duration.

### 2.5. Dimensionless variables

The dimensionless concentration, mass flux, wave speed, distance, time, and delay time, and a characteristic system parameter are defined, respectively, as follows:

$$c_D = \frac{c - c_0}{c^* - c_0}, \quad (2.18)$$

$$J_D = \frac{IJ}{D}, \quad (2.19)$$

$$\nu_D = \frac{L\nu}{D}, \quad (2.20)$$

$$x_D = \frac{x}{L}, \quad (2.21)$$

$$t_D = \frac{Dt}{L^2}, \quad (2.22)$$

$$\tau_D = \frac{D\tau}{L^2}, \quad (2.23)$$

$$k_D \equiv kL/D. \quad (2.24)$$

The parameter  $k_D$  can be referred to as a mass-transfer Biot number because of its analogy with heat-transfer problems.

In terms of the nondimensional variables, the mass-accumulation function  $Q(t)$  given by Eq. (2.8) can be expressed as the dimensionless average of the gas concentration  $Q_D(t_D)$  in the heterogeneous medium:

$$Q_D(t_D) = \int_0^1 c_D(x_D, t_D) dx_D. \quad (2.25)$$

Also, by Eq. (2.6)

$$Q_D(t_D) = \int_0^{t_D} J_D(t_D)|_{x_D=0} dt_D, \quad t_D > 0. \quad (2.26)$$

In nondimensional terms, Eq. (2.7) can now be written as

$$\frac{MH}{RTL(c^* - c_0)} \left[ \frac{p_o}{Z_o} - \frac{p}{Z} \right] = Q_D(t_D). \quad (2.27)$$

Further, Eqs. (2.10) and (2.12)–(2.17) can be expressed in terms of the nondimensional variables, respectively, as the following:

$$\frac{\partial c_D}{\partial t_D} + \frac{\partial J_D}{\partial x_D} = 0, \quad 0 \leq x_D \leq 1, \quad t_D > 0, \quad (2.28)$$

$$\tau_D \frac{\partial^2 c_D}{\partial t_D^2} + \frac{\partial c_D}{\partial t_D} = \frac{\partial^2 c_D}{\partial x_D^2}, \quad 0 \leq x_D \leq 1, \quad t_D > 0, \quad (2.29)$$

$$\tau_D \frac{\partial^2 J_D}{\partial t_D^2} + \frac{\partial J_D}{\partial t_D} = \frac{\partial^2 J_D}{\partial x_D^2}, \quad 0 \leq x_D \leq 1, \quad t_D > 0. \quad (2.30)$$

$$v_D = 1/\sqrt{\tau_D}. \quad (2.31)$$

The initial conditions are given by:

$$c_D = 0, \quad \frac{\partial c_D}{\partial t_D} = 0, \quad J_D = 0, \quad \frac{\partial J_D}{\partial t_D} = 0, \quad 0 \leq x_D \leq 1, \quad t_D = 0. \quad (2.32)$$

The interface surface resistive gas mass-transfer boundary condition is given by:

$$J_D|_{x_D=0} = k_D c_D, \quad x_D = 0, \quad t_D > 0. \quad (2.33)$$

The sealed boundary condition prevailing at the bottom of the heterogeneous medium is given by:

$$J_D = 0, \quad x_D = 1, \quad t_D > 0. \quad (2.34)$$

### 3. Special solutions to the non-Fickian gas transfer model

When the gas transport in the heterogeneous medium involves a delay time, i.e.  $\tau \neq 0$ , special analytical solutions can be applied as follows for semi-infinite and finite-thickness heterogeneous medium regions, based on the analysis presented in Appendix A according to Civan and Rasmussen [4].

#### 3.1. Semi-infinite region

Eqs. (A.24) and (A.25) for the concentrations, and (A.27) and (A.28) for the mass fluxes, are the exact solutions for the limiting case where the solid-end wall of the test tank sealing the end of the heterogeneous medium has been removed to plus infinity. Thus for the wave problem no reflections are involved. A comparison of the concentrations for the wave-diffusion case (Eq. (A.24)) with the pure-diffusion case (Eq. (A.25)) is shown in Fig. 1 for  $k_D = 1$ ,  $\tau_D = 0$  and 0.1, and

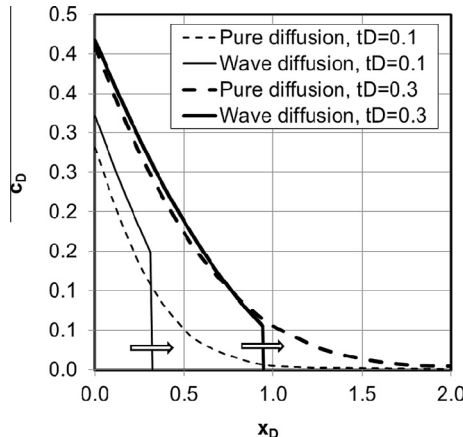


**Fig. 1.** Comparison of the non-dimensional concentration for wave diffusion ( $\tau_D = 0.1$ ) vs. pure diffusion ( $\tau_D = 0$ ) at the non-dimensional times  $t_D = 0.1$  and  $t_D = 0.3$  for  $k_D = 1$ .

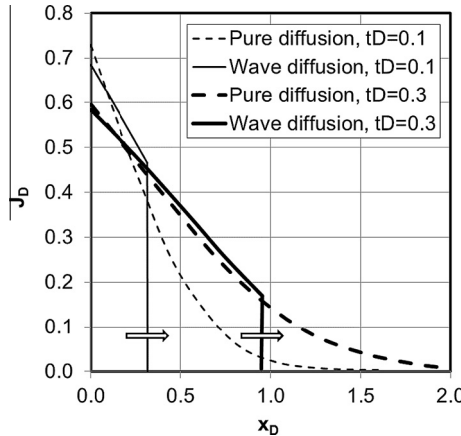


**Fig. 2.** Comparison of the non-dimensional diffusion flux for wave diffusion ( $\tau_D = 0.1$ ) vs. pure diffusion ( $\tau_D = 0$ ) at the non-dimensional times  $t_D = 0.1$  and  $t_D = 0.3$  for  $k_D = 1$ .

$t_D = 0.1$  and  $0.3$ . Fig. 2 shows a similar comparison for the diffusion fluxes, Eqs. (A.27) and (A.28). For  $\tau_D \neq 0$ , a discontinuity wave front propagates into the medium with the nondimensional speed  $v_D = dx_D/dt_D = 1/\sqrt{\tau_D}$ , its strength decreasing with time. For small times, the differences between the two cases are significant, and depend on the value of  $\tau_D$ . For large enough times, the wave behavior dies out, and the wave solutions approach the equilibrium pure-diffusion solutions, except very near the decaying wave front.

Consider now the diffusion flux at the interface,  $x_D = 0$ , as a function of time. Eq. (A.27) for the dimensionless diffusion flux becomes

$$\frac{1}{k_D} \cdot J_{D_b}(0, t_D) = -C_2(0, t_D) + C_3(0, t_D) - C_4(0, t_D), \quad (3.1)$$

where the functions  $C_2$ ,  $C_3$ , and  $C_4$  are defined in Appendix A.

The diffusion flux for the pure-diffusion case becomes

$$\frac{1}{k_D} [J_{D_b}(0, t_D)]_{\tau_D=0} = e^{k_D^2 t_D} \operatorname{erfc}(k_D \sqrt{t_D}). \quad (3.2)$$

Notice that the right side of the pure-diffusion case Eq. (3.2) is function of only the combination  $k_D^2 t_D$ . Fig. 3 shows a comparison of the interface diffusion fluxes for  $k_D = 1$  and  $\tau_D = 0, 0.2$ , and  $0.5$ . The values at  $t_D = 0$  are in agreement with Eq. (A.30). The wave-diffusion curves merge with the pure-diffusion curve approximately at  $t_D = 2\tau_D$ . This is suggested also from a perusal of the right side of the wave-diffusion function Eq. (3.1), which shows a functional dependence on the two groups  $k_D \sqrt{t_D}$  and  $t_D/2\tau_D$ .

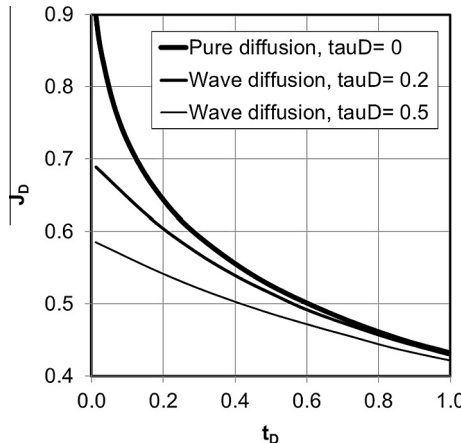


**Fig. 3.** Diffusion flux at the gas-heterogeneous medium interface ( $x_D = 0$ ) vs. time for comparison of the wave diffusion ( $\tau_D \neq 0$ ) vs. pure diffusion ( $\tau_D = 0$ ) for  $k_D = 1$ .

### 3.2. Mass-accumulation function

Consider now the function  $Q_{D_1}(t_D)$ , which describes in nondimensional form the cumulative amount of mass of gas absorbed by the heterogeneous medium, per unit area. For the first-order result, we have from the inversions of Eqs. (A.11) and (A.15)

$$Q_{D_1}(t_D) = \int_0^{t_D} J_{D_b}(0, \bar{t}_D) d\bar{t}_D. \quad (3.3)$$

This formula amounts to calculating the area under any one of the curves such as appearing in Fig. 3. Alternatively, we can work directly with the Laplace transform Eq. (A.15), which we can rearrange algebraically to read

$$\bar{Q}_{D_1}(s) = \frac{k_D}{s(bs + k_D^2)} \left[ (k_D \sqrt{\tau_D} - 1) + k_D \left\{ \frac{\sqrt{\tau_D s + 1}}{\sqrt{s}} - \sqrt{\tau_D} \right\} \right] \quad (3.4)$$

In this form, Laplace-transform tables can be used for inversion, and we get

$$k_D \cdot Q_{D_1}(t_D) = (k_D \sqrt{\tau_D} - 1) \left[ 1 - e^{-\frac{k_D^2 t_D}{b}} \right] + Q_1(t_D), \quad (3.5)$$

where

$$Q_1(t_D) \equiv k_D \sqrt{\tau_D} \int_0^{\frac{t_D}{2\tau_D}} \left\{ 1 - e^{-\frac{2k_D^2 \tau_D}{b} \left( \frac{t_D}{2\tau_D} - x \right)} \right\} e^{-x} (I_1(x) + I_o(x)) dx. \quad (3.6)$$

The right sides of Eqs. (3.5) and (3.6) show a functional dependence on the two groups  $k_D \sqrt{\tau_D}$  and  $t_D/2\tau_D$ . The pure-diffusion case can be obtained by inverting Eq. (A.15) directly with  $\tau_D = 0$ :

$$k_D \cdot [Q_{D_1}(t_D)]_{\tau_D=0} = e^{k_D^2 t_D} \operatorname{erfc}(k_D \sqrt{t_D}) - 1 + 2k_D \sqrt{\frac{t_D}{\pi}}. \quad (3.7)$$

Finally, it is useful to note the following asymptotic expansion for  $Q_{D_1}(t_D)$  for the pure-diffusion case when  $k_D \sqrt{t_D}$  is large:

$$k_D \cdot [Q_{D_1}(t_D)]_{\tau_D=0} \cong 2k_D \sqrt{\frac{t_D}{\pi}} - 1 + \frac{1}{k_D \sqrt{\pi t_D}} + \dots, \quad k_D \sqrt{t_D} \rightarrow \infty. \quad (3.8)$$

It is interesting to generalize this result by working with Eq. (A.17) and expanding it in an asymptotic expansion for small  $s$ :

$$\bar{Q}_{D_1}(s) \cong \frac{1}{s^{3/2}} - \frac{1}{k_D} \cdot \frac{1}{s} + \left( \frac{1}{k_D^2} - \frac{\tau_D}{2} \right) \cdot \frac{1}{\sqrt{s}} + \dots, \quad s \rightarrow 0 \quad (3.9)$$

Inversion term by term now gives the asymptotic expansion for large  $t_D$ :

$$Q_{D_1}(t_D) \cong 2 \sqrt{\frac{t_D}{\pi}} - \frac{1}{k_D} + \left( \frac{1}{k_D^2} - \frac{\tau_D}{2} \right) \frac{1}{\sqrt{\pi t_D}} + \dots, \quad t_D \rightarrow \infty. \quad (3.10)$$

The non-Fickian time constant  $\tau_D$  does not appear until the third term, which becomes vanishing small as  $t_D \rightarrow \infty$ .

Fig. 4 shows a comparison of the first-order mass-accumulation function  $Q_{D_1}(t_D)$  for the equilibrium pure-diffusion case  $\tau_D = 0$  versus the two non-Fickian wave-diffusion cases  $\tau_D = 0.3$  and  $0.6$ , and all cases for  $k_D = 1$ . The curves are plotted as a function of  $\sqrt{t_D}$  to show their relation with the two-term asymptote curve of Eqs. (3.8) and (3.10). Because the interface wave-diffusion curves in Fig. 3 all merge with the pure-diffusion curve after a time, the areas underneath them differ by a constant in due time. This is reflected in Fig. 4 by a nearly constant displacement after due time. Nevertheless, as Eq. (3.10) indicates, all the curves become asymptotic to the straight-line asymptote curve for very large times. The pure-diffusion curve differs from the asymptote curve by a factor of  $1/(k_D \sqrt{\pi t_D})$  when  $t_D$  is large, and this factor is not small for the results shown in the figure.

### 3.3. Finite-thickness region

The first approximations for the finite-thickness case, as can be gleaned from Eqs. (A.13) and (A.14), are

$$c_{D_1}(x_D, t_D) = c_{D_b}(x_D, t_D) + c_{D_b}(2 - x_D, t_D), \quad (3.11)$$

$$J_{D_1}(x_D, t_D) = J_{D_b}(x_D, t_D) - J_{D_b}(2 - x_D, t_D). \quad (3.12)$$

The first terms on the right sides are the basic right-running waves given by Eqs. (A.24) and (A.27). The second terms are the “image” left-running waves that start at  $x_D = 2$  and run to the left. In the case of pure diffusion,  $\tau_D = 0$ , the first functions start at  $x_D = 0$  and spread to the right, and the second functions start at  $x_D = 2$  and spread to the left. It takes both waves the

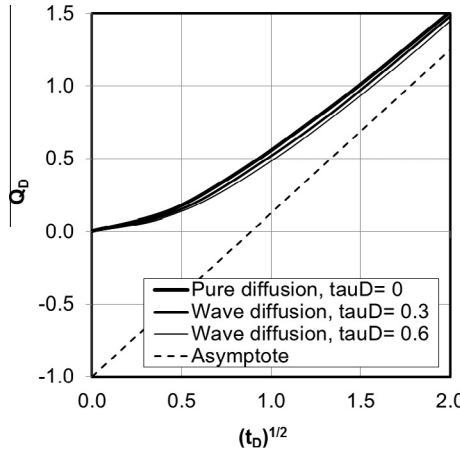


**Fig. 4.** Comparison of the mass-accumulation factor for the wave diffusion ( $\tau_D \neq 0$ ) vs. pure diffusion ( $\tau_D = 0$ ) for  $k_D = 1$ .

time interval  $t_D = \sqrt{\tau_D}$  to reach the solid wall at  $x_D = 1$ , and thereafter they begin to interact. The concentration waves, Eq. (3.11), are additive. The diffusion fluxes, Eq. (3.12), are subtractive, which satisfies the zero net flux condition at the wall. Thus the solution behavior for times less than  $t_D = \sqrt{\tau_D}$  is the same as the semi-infinite medium because the initial right-running wave has not yet reached the wall where the interaction begins. As we are only interested in the interval  $0 \leq x_D \leq 1$ , we can interpret the interaction of the right-running wave at the wall with the left-running wave, as the right-running wave's being “reflected” and becoming a left-running wave. It then takes the left-running reflected wave another time interval of  $t_D = \sqrt{\tau_D}$  to reach the interface at  $x_D = 0$ . Thus the total time that the first approximation is valid is  $t_D = 2\sqrt{\tau_D}$ . The waves described by the second approximation, Eqs. (A.16) and (A.17), come into play after this.

The situation for pure diffusion  $\tau_D = 0$  is not so clear-cut. We can, however, interpret the spreading of diffusion as having an infinite wave speed, but having zero wave strength. In fact the wave strength is exponentially small. Thus, although diffusion spreading immediately interacts, the interaction is initially very small, and many interpretations of the wave interactions hold approximately.

The initial propagation of a right-running wave and its reflection from the wall is illustrated for the dimensionless concentrations and diffusion fluxes in Figs. 5 and 6 for  $k_D = 1$  and  $\tau_D = 0.1$ . In Fig. 5, the concentration distribution is shown behind the initial right-running wave after times  $t_D = 0.1, 0.2$ , and  $0.3$  before it impinges on the wall at time  $t_D = \sqrt{0.1} \approx 0.316$ . The location of the left-running reflected wave is shown for  $t_D = 0.4$ . Both the right-running wave and the reflected left-running wave increase the concentration as they pass by, but by a diminishing amount as they travel along. The corresponding situation for the diffusion flux is shown in Fig. 6. The right-running wave is shown at  $t_D = 0.2$  and the reflected left-running wave at  $t_D = 0.35$ . The right-running wave increases the diffusion flux, but the left-running wave decreases the diffusion flux. The left-running diffusion wave reduces the diffusion flux to zero at the wall, thus satisfying the boundary condition.

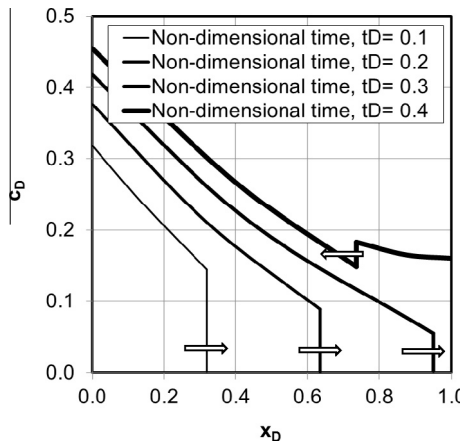


**Fig. 5.** Illustration of the reflected wave phenomena for the concentration in finite-thickness heterogeneous medium for  $\tau_D = 0.1$  and  $k_D = 1$ .

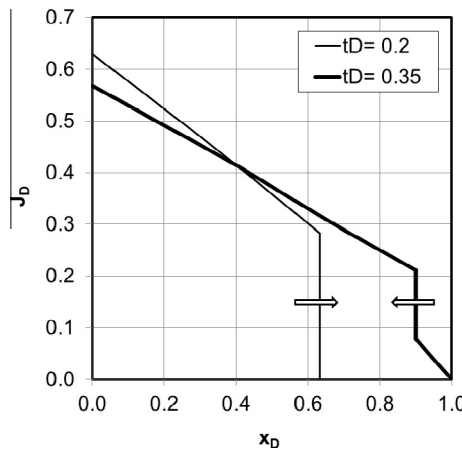


**Fig. 6.** Illustration of the reflected wave phenomena for the diffusion flux in finite-thickness heterogeneous medium for  $\tau_D = 0.1$  and  $k_D = 1$ .

The strengths of both the right-running and left-running waves diminish as they evolve with time. [Figs. 7 and 8](#) show the concentration and the diffusion-flux distribution for  $k_D = 1$  and  $\tau_D = 0.1$  as the reflected wave approaches the interface at time  $t_D = 0.6$ . In both cases, the conditions ahead of the wave have become nearly the same as for the pure-diffusion case with  $\tau_D = 0$ . The wave causes this concentration to jump to a value somewhat less than the pure-diffusion case, and the difference will soon decay away analogously to that in front of the wave. On the other hand, the wave causes the diffusion flux to decrease to a value somewhat greater than the pure-diffusion case, and this difference can be expected to soon decay away also.

These examples show that, after a time  $t_D = 2\sqrt{\tau_D}$ , the concentrations and diffusion fluxes will evolve nearly to those described by the pure-diffusion analysis. It is thus of interest to investigate the diffusion flux at the interface by the pure-diffusion case and to compare the results of the first approximation for the finite-thickness region with that of the semi-infinite region. This is shown in [Fig. 9](#) for  $k_D = 1$ . For small times, the results are the same, but for longer times the diffusion flux at the interface is less for the finite-thickness region. It is expected that upgrading the analysis to include the second approximation described in [Appendix A](#) would further enhance this result. Because the area under these curves represents the cumulative mass absorbed by diffusion, one might expect  $Q_D(t_D)$  to grow at a slower rate and to reach a limit as the finite-thickness region reaches equilibrium and “fills up”, rather than grow unbounded like  $\sqrt{t_D}$  for the semi-infinite medium.

### 3.4. Large-time approximation

For the non-Fickian case for the finite region, a large-time approximation cannot be found that rigorously links the initial condition, analogous to that given by Rasmussen and Civan [\[4\]](#) for the pure-diffusion problem. Some partial results are presented in the following but this issue is alleviated in a practical manner by the procedure presented in the next section.

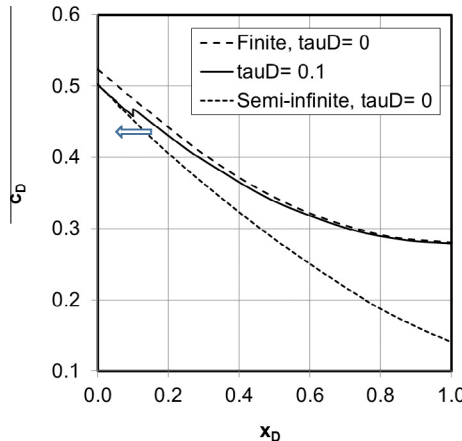


**Fig. 7.** Illustration of the reflected wave phenomena for concentration as it approaches the gas-heterogeneous medium interface for  $k_D = 1$  and  $t_D = 0.6$ .

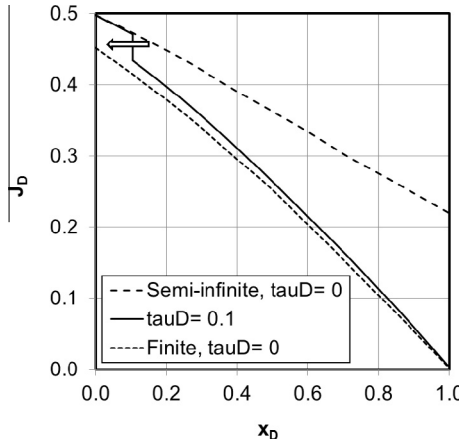


**Fig. 8.** Illustration of the reflected wave phenomena for diffusion flux as it approaches the gas–heterogeneous medium interface for  $k_D = 1$  and  $t_D = 0.6$ .

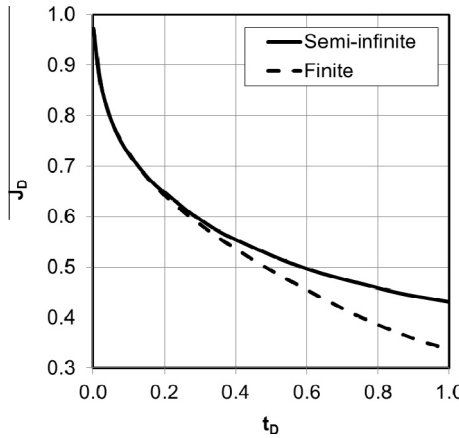


**Fig. 9.** Comparison of the pure diffusion fluxes at the gas–heterogeneous medium interface for semi-infinite and finite thickness heterogeneous medium for  $\tau_D = 0$  and  $k_D = 1$ .

We assume a separation-of-variables solution to Eq. (2.29) of the form

$$c_D(x_D, t_D) = 1 - X(x_D)e^{-\omega^2 t_D}. \quad (3.13)$$

Substituting this into Eq. (2.12) and canceling the time-exponential terms, we get

$$X'' + (\omega^2 - \tau_D \omega^4)X = 0. \quad (3.14)$$

Now make the definition

$$\lambda^2 = \omega^2 - \tau_D \omega^4. \quad (3.15)$$

Solving for  $\omega^2$  as a function of  $\lambda^2$ , we get

$$\omega^2 = \frac{2\lambda^2}{1 + \sqrt{1 - 4\tau_D \lambda^2}}. \quad (3.16)$$

The sign in front of the radical was chosen such that the pure diffusion case was recovered when  $\tau_D = 0$ . With the assumption that  $\lambda$  is real, the solution to Eq. (3.14) can be written

$$X = A \cos[\lambda(1 - x_D)] + B \sin[\lambda(1 - x_D)], \quad (3.17)$$

where  $A$  and  $B$  are arbitrary constants. Similar results can be fashioned for the diffusion mass flux  $J_D(x_D, t_D)$ . When the mass-conservation equation Eq. (2.28) and the end-wall no-flow condition Eq. (2.34) are satisfied, the results can be written as follows:

$$c_D = 1 - A \cos[\lambda(1 - x_D)] e^{-\omega^2 t_D}, \quad (3.18)$$

$$J_D = \frac{\omega^2}{\lambda} A \sin[\lambda(1 - x_D)] e^{-\omega^2 t_D}. \quad (3.19)$$

At this stage the constant  $A$  and the parameter  $\lambda$  remain to be specified.

In terms of the nondimensional variables, the interface boundary condition Eq. (2.33) can be expressed as

$$J_D(0, t_D) = k_D[1 - c_D(0, t_D)] \quad (3.20)$$

When expressions (3.18) and (3.19) are substituted into Eq. (3.20), we obtain

$$\begin{aligned} \frac{\omega^2}{\lambda} \tan \lambda &= k_D, \text{ or} \\ \frac{2 \lambda \tan \lambda}{1 + \sqrt{1 - 4 \tau_D \lambda^2}} &= k_D. \end{aligned} \quad (3.21)$$

This reduces to the pure-diffusion case Eq. (2.29) when  $\tau_D = 0$ .

The foregoing solution satisfies the governing equations and the two end boundary conditions, but it does not yet satisfy the initial condition, that is, the coefficient  $A$  in Eqs. (3.18) and (3.19) remains undetermined. The characteristic equation (3.21) for  $\lambda$  does not yield an infinite number of discrete roots that lend themselves to resolving the initial condition by means of a Fourier-series representation, as was the case for the pure-diffusion problem  $\tau_D = 0$  (Civan and Rasmussen [14–16,13]). In retrospect, perhaps, this is not surprising because the small-time behavior is inherently wave-like. Nevertheless, the wave behavior tends to die out rapidly, and it may be possible in some non-rigorous fashion join the large-time solution with the small-time solution by suitably choosing  $A$  (and possibly  $\lambda$  also).

With the coefficient  $A$  left undetermined, the cumulative-mass function can be obtained:

$$Q_D(t_D) = 1 - Q_o e^{-\omega^2 t_D}, \quad (3.22)$$

where

$$Q_o \equiv \frac{\sin \lambda}{\lambda} A \quad (3.23)$$

The constant  $A$  can in principle be found by the method of residues starting with the Laplace transform. This is left for future efforts. Nevertheless, this issue can be alleviated conveniently as described in the next section.

#### 4. Proposed method for non-Fickian data analysis

We wish to use Eq. (2.27) to interpret experimental data and infer from it the values of the diffusion coefficient  $D$  and the interface surface mass-transfer coefficient  $k$ . We assume that the quantities on the left side can all be measured or determined by some means such as demonstrated by Civan et al. [17,18], along with  $Q$  and thus the dimensionless mass-accumulation function  $Q_D$  as functions of time. The time function on the right side is assumed to represent the physical process involved and to thus correlate the data.

Let us suppose that equilibrium obtains after an effectively long time and that  $p$  equals  $p^*$ , the equilibrium pressure, when  $Q_D = 1$ . Then we have

$$\frac{M_g H}{RT_l(c^* - c_o)} \left[ \frac{p_o}{Z_o} - \frac{p^*}{Z^*} \right] = 1 \quad (4.1)$$

and Eq. (2.27) can be written as:

$$Q_D = \frac{\frac{p_o}{Z_o} - \frac{p}{Z}}{\frac{p_o}{Z_o} - \frac{p^*}{Z^*}}. \quad (4.2)$$

The right side can now be determined by measurement of pressure at a given temperature.

We consider the case for  $\tau_D = 0.1$  and  $k_D = 10$ . For this case, the time taken for the initial discontinuity wave to travel to the solid wall of the tank sealing the end of the heterogeneous medium and then reflect back and reach the interface between the gas and the heterogeneous medium is  $t_D^* = 2\sqrt{\tau_D} = 0.632$ . For times less than or equal to this, the small-time solution Eq. (3.6), which is shown in Fig. 10, is an exact solution. For  $t_D = t_D^* = 0.632$ , the mass accumulation is  $Q_D = Q_D^* = 0.767$ . According to the large-time analysis given in the preceding section, the large-time solution is (Eq. (3.22)):

$$Q_D(t_D) = 1 - Q_o e^{-\omega^2 t_D}, \quad (4.3)$$

where the constant  $Q_o$  is left undetermined. By means of the formulae given in the above section, it is found for this case that  $\omega^2 = 2.594 \cong 2.6$  and  $\lambda_1 = 1.326$ . If we now arbitrarily set the large-time solution equal to the small-time solution at  $t_D = 0.632$ , then  $Q_o$  can be determined as  $Q_o = 1.200$ . Then, the value of the constant  $A$  mentioned in Section 3 can be found using Eq. (3.23) as  $A = \frac{1.326(1.2)}{\sin(1.326)} = 1.64$ . The large-time solution so obtained is also shown in Fig. 10. The slopes of the two

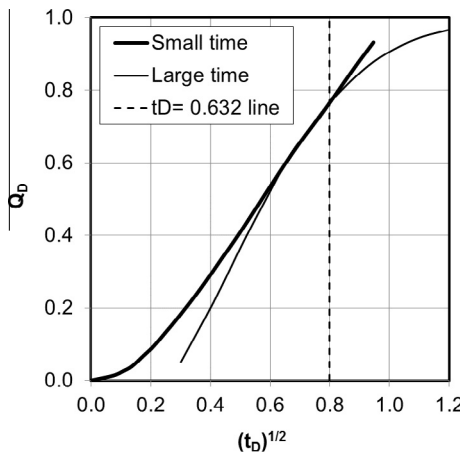


**Fig. 10.** Comparison of the small- and large-time approximations for plot of  $Q_D$  vs.  $\sqrt{t_D}$  for non-Fickian with  $\tau_D = 0.1$ ,  $k_D = 10$ .

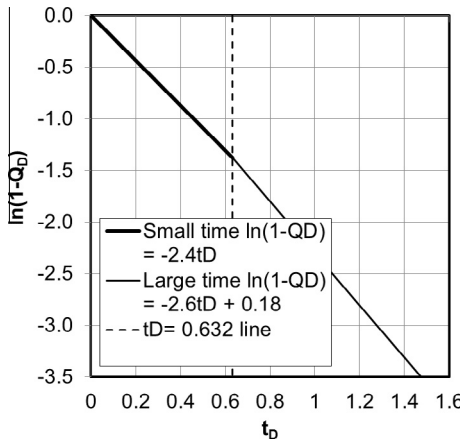


**Fig. 11.** Straight-line plots of  $\ln(1 - Q_D)$  vs  $t_D$  for the small- and large-time for non-Fickian with  $\tau_D = 0.1$ ,  $k_D = 10$  indicating a slope change from  $-2.4$  to  $-2.6$  at  $t_D = 0.632$ .

curves at the joining point are discontinuous, but this is reasonable owing to the wave nature of the problem. Note that on a semi-log plot given in Fig. 11, the value of the y-axis intercept would be positive.

The value of  $\tau_D = 0.1$  for this illustrative example is probably extremely high, and any real non-Fickian effects should have values of  $\tau_D$  considerably less than 0.1. Nevertheless, such nonFickian effects as studied here should be detectable experimentally. In fact, Fig. 11 is a plot of the  $\ln(1 - Q_D)$  vs  $t_D$  of the results given in Fig. 10 where the slopes of the straight-lines obtained for the small- and large-time for non-Fickian change from  $-2.4$  to  $-2.6$  at  $t_D = 0.632$ . It is interesting to note that such a break in the slope of this type was also observed in a similar plot of the experimental data by Smith and Fisher [12] for polymer exposed to water who attributed this behavior to the non-Fickian diffusion of water. Shankar [13] also made similar observation of a slope discontinuity. Hence, the results given in Fig. 11 is a reconfirmation of such characteristic behavior based on our analytical solution.

## 5. Applications and parameter determination

The estimation of the diffusion and interface surface mass-transfer coefficients, and the delay time based on the measurements obtained from the pressure decay tests conducted similar to Civan et al. [17,18] can be accomplished as proposed in the following. The methodology will be illustrated here by facilitating the results obtained from our analytical solutions as a substitute for actual experimental data. This course of action is taken because conduction of experimental studies is beyond the scope of the present paper. Thus, consider the results reported in Fig. 11 as a substitute for real experimental data which can be analyzed based on the following steps:

- (1) Determine the break between the small-time and large-time slopes from Fig. 11 as  $t_D^* = 0.632$  and  $Q_D^* = 0.767$ . Recall that the small-time analytical solution given by Eq. (3.6) is valid for  $t_D \leq t_D^*$  and the large-time analytical solution given by Eq. (3.22) is valid for  $t_D \geq t_D^*$  in the following calculations.
- (2) Determine the small-time slope as the following from Fig. 11 using Eq. (A.30) and applying  $Q_D(t_D) = 0$ ,  $t_D = 0$  according to Eq. (2.26):

$$\text{Slope}|_{t_D=0} = \frac{\partial \ln(1 - Q_D)}{\partial t_D} = \frac{-\frac{\partial Q_D(0,0)}{\partial t_D}}{1 - Q_D(0,0)} = \frac{-J_D(0,0)}{1 - Q_D(0,0)} = -J_D(0,0) = \frac{-k_D}{1 + k_D\sqrt{\tau_D}} = -2.4, \quad t_D = 0. \quad (4.4)$$

Thus, for small-times

$$\ln(1 - Q_D) \cong \frac{-k_D}{1 + k_D\sqrt{\tau_D}} t_D. \quad (4.5)$$

- (3) Determine the large-time slope as  $-\omega^2 = -2.594 \cong -2.6$  and intercept as  $\ln Q_o = 0.18$  so that  $Q_o = 1.2$  applying the following equation to Fig. 11 obtained from Eq. (3.22):

$$\ln[1 - Q_D(t_D)] = \ln Q_o - \omega^2 t_D. \quad (4.6)$$

- (4) Calculate  $\tau_D = (0.632/2)^2 = 0.1$  using the break point value  $t_D^* = 2\sqrt{\tau_D} = 0.632$ .
- (5) Calculate  $\lambda = \sqrt{\omega^2 - \tau_D\omega^4} = \sqrt{2.594 - 0.1(2.594)^2} = 1.326$  using Eq. (3.15).
- (6) Although, it is not necessary for determination of the diffusion and interface surface mass-transfer coefficients, the constant  $A$  mentioned in Sections 3 and 4 can be found using Eq. (3.23) as  $A = \frac{iQ_o}{\sin \lambda} = \frac{1.326(1.2)}{\sin(1.326)} = 1.64$ .
- (7) Calculate  $k_D = \frac{\omega^2}{\lambda} \tan \lambda = \frac{2.594}{1.326} \tan(1.326) \cong 10$  using Eq. (3.21).
- (8) Finally, the diffusion and interface surface mass-transfer coefficients can be calculated by Eqs. (2.23) and (2.24) respectively as  $D = \frac{l^2 \tau_D}{\tau} = \frac{l^2(0.1)}{\tau}$  and  $k = \frac{Dk_D}{L} = \frac{l \tau_D k_D}{L \tau} = \frac{l(0.1)(10)}{L \tau} = \frac{l}{\tau}$ . Hence, if, for example, the thickness of the heterogeneous media is given as  $L = 0.005$  m and the delay time as  $\tau = 10,000$  s = 2.78 h, then the values of the diffusion and interface surface mass-transfer coefficients can be calculated, respectively, as  $D = \frac{(0.005)^2(0.1)}{10000} = 2.5 \times 10^{-10}$  m<sup>2</sup>/s and  $k = \frac{0.005(0.1)(10)}{10000} = 5.0 \times 10^{-7}$  m/s. Note that the value of the delay time  $\tau$  can be determined if also the concentration profiles over the thickness of the heterogeneous medium similar to those shown in Figs. 1, 5 and 7 can be determined at various times with proper measurements. Unfortunately, however, such measurements have not been made for example by Smith and Fisher [12] in their experimental studies for testing of a polymer in water.

As stated previously, a third-order solution can be obtained by keeping three terms of the series in Eq. (A.12) from Eqs. (A.9)–(A.11), and even more terms to obtain higher-order solutions. However, as demonstrated here, our low-order approximate solutions capture upon the dominant features of the non-Fickian diffusion problem adequately. Although the addition of more terms can certainly improve the accuracy, their contributions diminish progressively as the order of the terms increases in the series expansion used in this paper. For purposes of this paper our approximate solutions are sufficiently accurate and allow for adequate analysis of data.

The above exercise demonstrates the application of the analytical methodology required for description of the non-Fickian gas dissolution in heterogeneous medium and estimation of the diffusion and interface surface mass-transfer coefficients from measured pressure decay data. As stated before this was the overall objective of this paper and therefore the applications of this approach for analyses of the experimental data of specific cases of practical interest are reserved to future studies.

Nevertheless, some “partial” data are available from Smith and Fisher [12] and Zaki et al. [19]. Smith and Fisher [12] obtained the experimental data for a cellulose-filled polymer (68% cross-linked melamine-formaldehyde resin) exposed to water at 95 °C and Zaki et al. [19] obtained the experimental data for the copolymer polypropylene (83% propylene and 17% methylene monomers) exposed to a 50,000 ppm aqueous solution of amyl acetate at 40 °C temperature. Both of these polymers are used as packing materials. Galdamez et al. [20] obtained the experimental data by exposing 2.84 g chocolate sample to 1.14 g hazelnut oil at 23 °C temperature. These data are sufficient to determine both the small- and large-time slopes; unfortunately, however, no data are provided by these studies which are required for determination of the delay time involved in their specific cases. The latter requires the matching of the model responses to the concentration profiles of the diffusing species in the samples measured at various times during the tests.

Fig. 12 presents the straight-line plots of  $\ln(1 - Q_D)$  vs  $t$  for the small- and large-time for non-Fickian data of Smith and Fisher [12] indicating a slope change from  $-0.096$  to  $-0.2232$  at  $t = 14$  h. Fig. 13 presents the similar plots for non-Fickian data of Zaki et al. [19] indicating a slope change from  $-0.009$  to  $-0.0207$  at  $t = 19$  h. Fig. 14 presents the straight-line plots of  $\ln(1 - Q_D)$  vs  $t$  for the small- and large-time for non-Fickian data of Galdamez et al. [20] indicating a slope change from  $-0.0386$  to  $-0.021$  at  $t = 50$  h. The determination of the delay time as well as the diffusion and interface surface mass-transfer coefficients would have been possible had also the concentration profiles of the diffusing species in the heterogeneous samples been measured at various times during the tests. Therefore, future studies should consider such measurements by appropriate means.

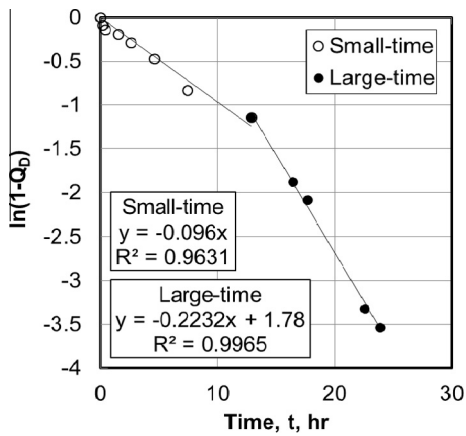


**Fig. 12.** Straight-line plots of  $\ln(1 - Q_D)$  vs  $t$  for the small- and large-time for non-Fickian data of Smith and Fisher [12] indicating a slope change from  $-0.096$  to  $-0.2232$  at  $t = 14$  h.

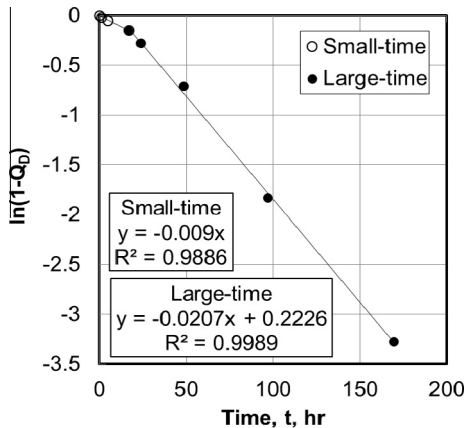


**Fig. 13.** Straight-line plots of  $\ln(1 - Q_D)$  vs  $t$  for the small- and large-time for non-Fickian data of Zaki et al. [19] indicating a slope change from  $-0.009$  to  $-0.0207$  at  $t = 19$  h.

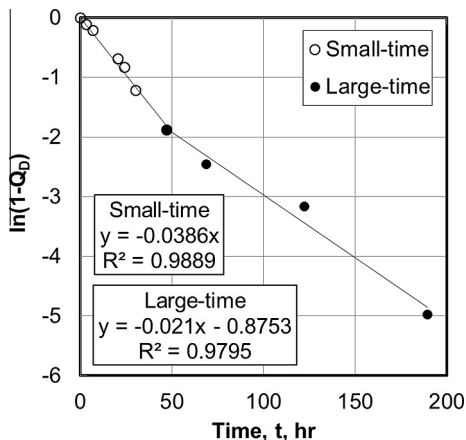


**Fig. 14.** Straight-line plots of  $\ln(1 - Q_D)$  vs  $t$  for the small- and large-time for non-Fickian data of Galdamez et al. [20] indicating a slope change from  $-0.0386$  to  $-0.021$  at  $t = 50$  h.

## 6. Concluding remarks

The analytical approach presented in this paper provides valuable insights into the mechanism of the non-Fickian gas diffusion with delay processes, and the role that the delay time, the diffusion coefficient of gas in heterogeneous medium, and the interface surface mass-transfer coefficient play in gas transfer involving heterogeneous medium.

Based on the analytical studies conducted in this paper, we can make the following conclusions:

- Full-, short-, and long-time analytical solutions were generated successfully for transient-state non-Fickian diffusion of gas in locally heterogeneous medium suddenly exposed to high pressure gas under isothermal conditions.
- Comparison of the concentrations for the wave-diffusion case with the pure-diffusion case demonstrated the significance of the non-Fickian gas dissolution in heterogeneous medium.
- Special analytical solutions were developed and applied for semi-infinite and finite-thickness regions for gas transport in heterogeneous medium with delay. The propagation of a right-running wave and its reflection from the wall was illustrated for the concentrations and diffusion fluxes.
- The small-time behavior was shown to be wave-like with a discontinuity wave front propagating into the medium with a speed diminishing with time. For small times, the differences between the wave-diffusion and the pure-diffusion cases were found to be significant depending on the value of the delay time.
- For sufficiently large times, the wave behavior dies out and the wave solutions approach the equilibrium pure-diffusion solutions, except for very near the decaying wave front.
- Our analytical solution reconfirmed the experimentally observed occurrence of a break in the slopes of the straight-lines obtained for the small- and large-times in a plot of  $\ln(1 - Q_D)$  vs  $t_D$  or  $t$  based on the data obtained during the tests of polymer exposed to water by Smith and Fisher [12], the copolymer polypropylene exposed to aqueous solution of amyl acetate by Zaki et al. [19], and the chocolate samples exposed to hazelnut oil by Galdamez et al. [20].
- The formulations presented in this paper are of practical importance because they can be used also for determination of the diffusivity, interface surface-mass-transfer coefficient, and rate of dissolution of gases in heterogeneous medium.
- Thus, investigations by meaningful experimental measurement techniques are recommended for future studies, such as the pressure-pulse decay method similar to Civan et al. (2012), for which the data measured under non-Fickian conditions, can be analyzed by applying the present analytical solutions. However, the determination of the delay time requires also the measurements of the concentration profiles of the diffusing species in the samples at various times during the tests.

## Acknowledgment

Parts of this study have been reprinted with modifications from the authors' previous study: "Civan, F. and Rasmussen, M.L., Analysis and Interpretation of Gas Diffusion in Quiescent Reservoir, Drilling, and Completion Fluids: Equilibrium vs. Nonequilibrium Models, Paper SPE 84072 presented at the Society of Petroleum Engineers Annual Technical Conference and Exhibition, Denver, Colorado, 5–8 October 2003". The authors thank for the permission.

## Appendix A. Analytical solutions to the dimensionless non-Fickian gas transfer model

The analytical solution of the non-Fickian gas diffusion problem (Eqs. (2.25)–(2.34)) is presented in the following in terms of the dimensionless variables and parameters.

### A.1. Laplace-transform analysis

The Laplace transform of Eq. (2.30) with respect to the time  $t_D$ , accounting for the initial conditions Eq. (2.32), is

$$\bar{J}_{Dxx} - (\tau_D s^2 + s)\bar{J}_D = 0, \quad (\text{A.1})$$

where  $\bar{J}_D(x_D, s)$  denotes the transform of  $J_D(x_D, t_D)$ . Solving the ordinary differential equation (A.1) yields:

$$\bar{J}_D(x_D, s) = Ae^{-x_D q} + Be^{+x_D q}, \quad (\text{A.2})$$

where A and B are arbitrary constants and define

$$q \equiv \sqrt{\tau_D s^2 + s}. \quad (\text{A.3})$$

Imposing the boundary condition, Eq. (2.34), at  $x_D = 1$  yields

$$B = -Ae^{-2q} \quad (\text{A.4})$$

and therefore we have

$$\bar{J}_D(x_D, s) = A[e^{-x_D q} - e^{-(2-x_D)q}]. \quad (\text{A.5})$$

To impose the boundary condition at the interface  $x_D = 0$ , we must first establish the transform of the concentration  $c_D$ . The transform of Eq. (2.28) yields:

$$\bar{c}_D(x_D, s) = -\frac{\bar{J}_{Dx}(x_D, s)}{s}. \quad (\text{A.6})$$

Thus we have

$$\bar{c}_D(x_D, s) = A \frac{q}{s} [e^{-x_D q} + e^{-(2-x_D)q}]. \quad (\text{A.7})$$

The transform of the boundary condition, Eq. (2.33), at the interface  $x_D = 0$  now yields the constant  $A$ :

$$A = \frac{k_D}{(1 + \frac{q}{s} k_D) - (1 - \frac{q}{s} k_D) e^{-2q}}. \quad (\text{A.8})$$

With  $A$  determined, the transforms  $\bar{c}_D$  and  $\bar{J}_D$  can now also be determined as:

$$\bar{c}_D(x_D, s) = \frac{k_D}{s} \cdot \frac{e^{-qx_D} + e^{-q(2-x_D)}}{\left(\frac{s}{q} + k_D\right) - \left(\frac{s}{q} - k_D\right) e^{-2q}}, \quad (\text{A.9})$$

$$\bar{J}_D(x_D, s) = \frac{k_D}{s} \cdot \frac{e^{-qx_D} - e^{-q(2-x_D)}}{(1 + \frac{q}{s} k_D) - (1 - \frac{q}{s} k_D) e^{-2q}}. \quad (\text{A.10})$$

We are also interested in the mass-accumulation function  $Q_D$ , the Laplace transform of which is obtained by integrating Eq. (A.9) with respect to  $x_D$  in accordance with Eq. (2.25). We have

$$\bar{Q}_D(s) = \frac{k_D}{s} \cdot \frac{1 - e^{-2q}}{(s + k_D q) - (s - k_D q) e^{-2q}} = \frac{1}{s} \bar{J}_D(0, s). \quad (\text{A.11})$$

The inversion of these Laplace transforms now remains.

#### A.2. Inversion for small times

The small-time approximation corresponds to large  $s$ . In this limit, the term with the exponential in the denominator is small compared to the first, and for the terms in the denominator of Eq. (A.9) we can thus write

$$\frac{1}{\left(\frac{s}{q} + k_D\right) - \left(\frac{s}{q} - k_D\right) e^{-2q}} = \frac{1}{\left(\frac{s}{q} + k_D\right) \left[1 - \left(\frac{s-qk_D}{s+qk_D}\right) e^{-2q}\right]} = \frac{\sum_{n=0}^{\infty} \left(\frac{s-qk_D}{s+qk_D}\right)^n e^{-2nq}}{\frac{s}{q} + k_D}. \quad (\text{A.12})$$

A binomial expansion was used to obtain the series. The series involved is always convergent.

#### A.3. Lowest-order approximation

The lowest-order (or first-order) small-time approximation occurs when only the first term in the series is retained. Thus we have from Eqs. (A.9)–(A.11)

$$\bar{c}_{D1}(x_D, s) = \frac{k_D}{s} \cdot \frac{e^{-qx_D} + e^{-q(2-x_D)}}{\frac{s}{q} + k_D}, \quad (\text{A.13})$$

$$\bar{J}_{D1}(x_D, s) = \frac{k_D}{s} \cdot \frac{e^{-qx_D} - e^{-q(2-x_D)}}{1 + \frac{q}{s} k_D}, \quad (\text{A.14})$$

$$\bar{Q}_{D1}(s) = \frac{k_D}{s} \cdot \frac{1}{s + k_D q}. \quad (\text{A.15})$$

For  $\tau_D \neq 0$ , the results (A.13) and (A.14) show a wave behavior. The first exponential term generates a damped discontinuity wave, starting at  $x_D = 0$  and traveling in the positive  $x_D$  direction (right-running wave). The second exponential term generates a damped discontinuity “image” wave that starts at  $x_D = 2$  and travels in the negative  $x_D$  direction (left-running wave). The two waves meet at  $x_D = 1$ , canceling each other to enforce the solid-wall boundary condition  $\bar{J}_D(x_D = 1, s) = 0$ , and reinforcing each other to form an apparent jump in the value of the concentration at the wall when the waves meet. Because the problem is essentially posed in the range  $0 \leq x_D \leq 1$ , the “image” wave is inconsequential, and the right-running

wave appears to be “reflected” from the wall at  $x_D = 1$ , and becomes a left-running wave. The reflected wave continues leftward until it impinges on the interface surface at  $x_D = 0$ , and the first-order solutions (Eqs. (A.13)–(A.15)) cease to be valid for further development. In view of the wave nature of the problem, and of the wave speed given by Eq. (2.31), the first-order solution is valid and is in fact an exact solution when  $t_D < 2\sqrt{\tau_D}$ .

The second-order solution describes the subsequent pair of events after the left-running reflected wave is reflected from the interface as a right-running wave, which eventually is reflected from the wall as another left-running wave. The second-order solution is obtained by keeping two terms of the series in Eq. (A.12). Thus, we now have have from Eqs. (A.9)–(A.11):

$$\bar{c}_{D_2}(x_D, s) = \bar{c}_{D_1}(x_D, s) + \frac{k_D}{s} \left( \frac{s - qk_D}{s + qk_D} \right) \frac{e^{-q(2+x_D)} + e^{-q(4-x_D)}}{\frac{s}{q} + k_D}, \quad (\text{A.16})$$

$$\bar{J}_{D_2}(x_D, s) = \bar{J}_{D_1}(x_D, s) + \frac{k_D}{s} \left( \frac{s - qk_D}{s + qk_D} \right) \frac{e^{-q(2+x_D)} - e^{-q(4-x_D)}}{1 + \frac{q}{s} k_D}, \quad (\text{A.17})$$

$$\bar{Q}_{D_2}(s) = \bar{Q}_{D_1}(s) - \frac{k_D}{s} \left( \frac{2k_D q}{s + k_D q} \right) \frac{e^{-2q}}{s + k_D q}. \quad (\text{A.18})$$

A third-order solution is obtained correspondingly by keeping three terms of the series in Eq. (A.12) from Eqs. (A.9)–(A.11), and so on for the higher-order solutions.

#### A.4. Inversion of first-order approximation

The inversion of Eqs. (A.13)–(A.15) can be facilitated if the following identity is noted:

$$\left[ \frac{1}{s} \right] \left[ \frac{1}{\frac{s}{q} + k_D} \right] \equiv \frac{1}{k_D} \left[ \frac{1}{s} + \frac{1}{k_D^2 + bs} \right] - \frac{1}{bq} \left[ \tau_D - \frac{1}{k_D^2 + bs} \right] \quad (\text{A.19})$$

where  $b \equiv \tau_D k_D^2 - 1$ . The four terms on the right side of Eq. (A.19), when multiplied by  $e^{-qx_D}$ , admit to inversion by means of standard Laplace-transform tables. The four inversions lead to the following four respective functions (for  $b \neq 0$ ):

$$C_1(x_D, t_D) \equiv \exp \left( -\frac{x_D}{2\sqrt{\tau_D}} \right) H(t_D - x_D \sqrt{\tau_D}) + \frac{x_D}{2\sqrt{\tau_D}} \int_0^{t_D} \frac{e^{-\frac{t}{2\tau_D}} H(t - x_D \sqrt{\tau_D}) \cdot I_1 \left( \frac{\sqrt{t^2 - x_D^2 \tau_D}}{2\tau_D} \right) dt}{\sqrt{t^2 - x_D^2 \tau_D}}, \quad (\text{A.20})$$

$$C_2(x_D, t_D) = \frac{\exp \left[ -\frac{x_D}{2\sqrt{\tau_D}} - \frac{k_D^2(t_D - x_D \sqrt{\tau_D})}{\tau_D k_D^2 - 1} \right]}{\tau_D k_D^2 - 1} \cdot H(t_D - x_D \sqrt{\tau_D}) + \frac{x_D e^{-\frac{t_D}{\tau_D k_D^2 - 1}}}{2\tau_D(\tau_D k_D^2 - 1)} \cdot \int_0^{t_D} \frac{e^{\left( \frac{k_D^2 t}{\tau_D k_D^2 - 1} - \frac{t}{2\tau_D} \right)} H(t - x_D \sqrt{\tau_D})}{\sqrt{t^2 - x_D^2 \tau_D}} \\ \cdot I_1 \left( \frac{\sqrt{t^2 - x_D^2 \tau_D}}{2\tau_D} \right) dt, \quad (\text{A.21})$$

$$C_3(x_D, t_D) \equiv \frac{k_D \sqrt{\tau_D}}{\tau_D k_D^2 - 1} \exp \left( -\frac{t_D}{2\tau_D} \right) \cdot I_0 \left( \frac{\sqrt{t_D^2 - x_D^2 \tau_D}}{2\tau_D} \right) H(t_D - x_D \sqrt{\tau_D}), \quad (\text{A.22})$$

$$C_4(x_D, t_D) \equiv \frac{k_D e^{\frac{k_D^2 t_D}{\tau_D k_D^2 - 1}}}{\tau_D(\tau_D k_D^2 - 1)^2} \cdot \int_0^{t_D} e^{\left( \frac{k_D^2 t}{\tau_D k_D^2 - 1} - \frac{t}{2\tau_D} \right)} I_0 \left( \frac{\sqrt{t^2 - x_D^2 \tau_D}}{2\tau_D} \right) \cdot H(t - x_D \sqrt{\tau_D}) dt, \quad (\text{A.23})$$

where  $I_0$  and  $I_1$  are the modified Bessel functions of the first kind, of order zero and one, and  $H(u)$  is the Heaviside unit step function, such that  $H(u) = 0$  when  $u < 0$  and  $H(u) = 1$  when  $u > 0$ .

Let us now consider the normalized concentration function  $c_D(x_D, t_D)$  defined by Eq. (2.18). This function varies between zero (at the initial condition) and unity (at the final equilibrium condition). The basic right-running wave corresponding to the first exponential term in Eq. (A.13) is

$$c_{D_b}(x_D, t_D) = C_1(x_D, t_D) + C_2(x_D, t_D) - C_3(x_D, t_D) + C_4(x_D, t_D). \quad (\text{A.24})$$

Setting  $\tau_D = 0$  in Eq. (A.13) and making the inversion accordingly yield the corresponding basic solution for the pure diffusion case as:

$$[c_{D_b}(x_D, t_D)]_{\tau_D=0} = \operatorname{erfc}\left(\frac{x_D}{2\sqrt{t_D}}\right) - e^{(k_D x_D + k_D^2 t_D)} \operatorname{erfc}\left(k_D \sqrt{t_D} + \frac{x_D}{2\sqrt{t_D}}\right). \quad (\text{A.25})$$

Expressions for the mass flux  $J_D$  can be developed in the following way. Note that

$$\frac{1}{1 + \frac{q}{s} k_D} \equiv 1 - \frac{k_D}{\frac{s}{q} + k_D}. \quad (\text{A.26})$$

Thus, the inversion of  $\bar{J}_D$  is related to the inversion of  $c_D$ , by comparison of Eqs. (A.16), (A.17) and (A.26). With this in mind, the first approximation, Eq. (A.17), can be inverted, starting with the right-running wave term involving the first exponential term, which we define as the basic solution:

$$\frac{1}{k_D} J_{D_b}(x_D, t_D) = C_1(x_D, t_D) - c_{D_b}(x_D, t_D) = -C_2(x_D, t_D) + C_3(x_D, t_D) - C_4(x_D, t_D). \quad (\text{A.27})$$

The functions involved have been previously defined by Eqs. (A.20)–(A.23), and (A.24). The corresponding result for the pure diffusion case is given by

$$\frac{1}{k_D} [J_{D_b}(x_D, t_D)]_{\tau_D=0} = \operatorname{erfc}\left(\frac{x_D}{2\sqrt{t_D}}\right) - [c_{D_b}(x_D, t_D)]_{\tau_D=0} = e^{(k_D x_D + k_D^2 t_D)} \operatorname{erfc}\left(k_D \sqrt{t_D} + \frac{x_D}{2\sqrt{t_D}}\right). \quad (\text{A.28})$$

It can be shown that the values of the concentration and the mass flux at the interface,  $x_D = 0^+$ , and immediately after the process starts,  $t_D = 0^+$ , are given by

$$c_{D_b}(0, 0) = \frac{k_D \sqrt{\tau_D}}{1 + k_D \sqrt{\tau_D}}, \quad (\text{A.29})$$

$$J_{D_b}(0, 0) = \frac{k_D}{1 + k_D \sqrt{\tau_D}}. \quad (\text{A.30})$$

## References

- [1] A.V. Luikov, Application of irreversible thermodynamics methods to investigation of heat and mass transfer, *Int. J. Heat Mass Transfer* 9 (2) (1966) 139–152.
- [2] S.L. Sobolev, *Sov. Phys. Uspekhi* 34 (1991) 217 (*Uspekhi Fiz. Nauk.* 5 (1991) 161).
- [3] I.I. Abarzhi, Wave mechanism of mass transfer for kinetics of adsorption in biporous medium, *J. Colloids Surf. A* 164 (2000) 105–113.
- [4] F. Civan, M.L. Rasmussen, Analysis and interpretation of gas diffusion in quiescent reservoir, drilling, and completion fluids: equilibrium vs. nonequilibrium models, Paper SPE 84072, SPE Annual Technical Conference and Exhibition, Denver, Colorado, 5–8 October 2003.
- [5] A.K. Das, A non-Fickian diffusion equation, *J. Appl. Phys.* 70 (3) (1991) 1355–1358.
- [6] P. Reverberi, P. Bagnerini, L. Maga, A.G. Bruzzone, On the non-linear Maxwell-Cattaneo equation with non-constant diffusivity: shock and discontinuity waves, *Int. J. Heat Mass Transfer* 51 (21–22) (2008) 5327–5332.
- [7] H.T. Chen, K.C. Liu, Analysis of non-Fickian diffusion problems in composite medium, *Comput. Phys. Commun.* 150 (2003) 31–42.
- [8] F. Civan, C.M. Sliepevich, Comparison of the thermal regimes for freezing and thawing of moist soils, *Water Resour. Res.* 21 (3) (1985) 407–410.
- [9] F. Civan, Unfrozen water content in freezing and thawing soils—kinetics and correlation, *J. Cold Regions Eng.* 14 (3) (2000) 146–156.
- [10] F. Liu, S.K. Bhatia, I.I. Abarzhi, Numerical solution of hyperbolic models of transport in bidisperse solids, *Comput. Chem. Eng.* 24 (2000) 1981–1995.
- [11] T. Vickerstaff, *The Physical Chemistry of Dyeing*, Imp. Chem. Ind., London, 1954.
- [12] P.M. Smith, M.M. Fisher, Non-Fickian diffusion of water in melamine-formaldehyde resins, *Polymer* 25 (1) (1984) 84–90, [http://dx.doi.org/10.1016/0032-3861\(84\)90271-4](http://dx.doi.org/10.1016/0032-3861(84)90271-4).
- [13] V. Shankar, Calculation of diffusion coefficients of organic vapours from short and longtime sorption data, *Polymer* 20 (2) (1979) 254–257.
- [14] F. Civan, M.L. Rasmussen, Determination of gas diffusion and interface-mass transfer coefficients for quiescent reservoir liquids, *SPE J.* 11 (1) (2006) 71–79.
- [15] F. Civan, M.L. Rasmussen, Rapid simultaneous evaluation of four parameters of single-component gases in nonvolatile liquid medium from a single data set, *Chem. Eng. Sci.* 64 (23) (2009) 5084–5092.
- [16] M.L. Rasmussen, F. Civan, Parameters of gas dissolution in liquid medium obtained by isothermal pressure decay, *AIChE J.* 55 (1) (2009) 9–23.
- [17] F. Civan, C.S. Rai, C.H. Sondergeld, Determining shale permeability to gas by simultaneous analysis of various pressure tests, Paper 144253-PA, *SPE J.* 17 (3) (2012) 717–726.
- [18] F. Civan, C.S. Rai, C.H. Sondergeld, Shale-gas permeability and diffusivity inferred by improved formulation of relevant retention and transport mechanisms, *Transp. Porous Media* 86 (3) (2011) 925–944.
- [19] O. Zaki, B. Abbes, L. Safa, Non-Fickian diffusion of amyl acetate in polypropylene packing: experiments and modelling, *Polym. Test.* 28 (2009) 315–323.
- [20] J.R. Galdemez, K. Szlachetka, J.L. Duda, G.R. Ziegler, Oil migration in chocolate: a case of non-Fickian diffusion, *J. Food Eng.* 92 (2009) 261–268.